Journal of Applied Polymer Science

Poly(ethylene terephthalate)/Poly(ethylene glycol-co-1,3/1,4-cyclohexanedimethanol terephthalate)/Clay Nanocomposites: Mechanical Properties, Optical Transparency, and Barrier Properties

Jyh-Horng Wu,[1] Ming-Shien Yen,[2] M. C. Kuo,[2] Yuhsin Tsai,[3] Ming-Tsong Leu[1]

[1]Material Application Center, Industrial Technology Research Institute, Tainan, Taiwan

[2]Department of Materials Engineering, Kun Shan University, Tainan, Taiwan

[3]School of Chinese Medicine, China Medical University, Taichung, Taiwan

Correspondence to: M. C. Kuo (E-mail: muchen@mail.ksu.edu.tw); Yuhsin Tsai (E-mail: yhtsai@mail.cmu.edu.tw)

Poly(ethylene terephthalate) (PET)/clay, PET/poly(ethylene glycol-co-1,3/1,4-cyclohexanedimethanol terephthalate) (PETG), and PET/PETG/clay nanocomposites were fabricated using the twin-screw extrusion technique. The spherulitic morphologies, thermomechanical, mechanical, and gas-barrier properties, as well as the effect of clay on the transparency of the resulting nanocomposites were identified. The clay induced the heterogeneous nucleation of the nanocomposites during the cold crystallization process, thereby increasing the crystallinities and melting temperatures of the resulting nanocomposites. The incorporation of clay increased the storage moduli, Young's moduli, impact strengths, and barrier properties of the PET, PETG, and PET/PETG blend. Regarding the optical transparency, the inclusion of clay can make the crystallizable PET matrix crystalline opaque. However, the amorphous PETG maintained its transparency. © 2013 Wiley Periodicals, Inc. J. Appl. Polym. Sci. **2014**, *131*, 39869.

KEYWORDS: PET; PETG; clay; barrier properties

Received 14 May 2013; accepted 20 August 2013

DOI: 10.1002/app.39869

INTRODUCTION

Poly(ethylene terephthalate) (PET) is an outstanding engineering polymer that has been used widely in food and beverage packaging applications. Recently, several researchers have reported that the incorporation of clay increases the gas-barrier properties of PET/clay nanocomposites.[1–5] Nevertheless, the crystallization rate of PET/clay nanocomposites exceeds that of PET, in which the clay is believed to act as a nucleating agent.[6–17] PET/clay nanocomposites are generally opaque due to high crystallinity arisen by the inclusion of clay. Thus, they are unsuitable under this condition for use in food and beverage packaging.

In contrast to semicrystalline PET polymers, poly(ethylene terephthalate-co-1,4-cyclohexylenedimethylene terephthalate (PETG) is an amorphous thermoplastic of the commercial PET family, with physical properties similar to PET.[18,19] In our previous study, we demonstrated that the amorphous nature of PETG would be unaffected by the inclusion of clay.[20] Instead, PETG has been found to form a miscible blend with PET.[21] Papadopoulou and Kalfoglou reported that the PET/PETG blend has a single endothermic peak in both T_g (93.3°C) and T_m (235.0°C) at a mixing ratio of 50/50 under the second heating run, indicating that this blend has good compatibility.[21]

In our previous study, the morphology and isothermal crystallization kinetics of PET/PETG/clay nanocomposites has been investigated.[22] Blending crystallizable PET with compatible and amorphous PETG could decrease the crystallinity and lower the crystallization rate of the PET segments, which improves the opaque problem. Accordingly, the PET/PETG/clay nanocomposites could possess the gas-barrier properties and maintain the transparency for food and beverage packaging. The objective of this study was to investigate the spherulitic morphologies, thermomechanical, mechanical, and gas-barrier properties, as well as the transparency of the PET/PETG/clay nanocomposites.

EXPERIMENTAL

Materials

The PET polymer (SHINPET 5015W) was kindly supplied by Shinkong Synthetic Fibers Co., Taiwan. PETG was prepared by two-stage melt-polycondensation (esterification and polycondensation) in an autoclave reactor. The molar ratio of ethylene glycol (EG)/1,3/1,4-cyclohexanedimethanol (1,3/1,4-CHDM) was 70/30. The details of the synthesis can be found in our previous study.[23] Cloisite 15A (aspect ratio: 75–100, quat concentration: 125 mequic/100 g, X-ray d_{001}: 3.14 nm, density: 1.66 g/cm^3) was purchased from Southern Clay Products. Cloisite 15A is a natural

Table I. Recipes for the Preparation of PET/PETG/Clay Nanocomposites (phr)

Composition	PET	PETG	Clay
PET	100	-	-
PETG	-	100	-
PET/PETG	50	50	-
PET/clay[a]	100	-	6
PETG/clay[a]	-	100	6
PET/PETG/clay[a]	50	50	6

[a] Clay was mixed with different aspect ratio of Cloisite 15A and MPGN in 1 : 1 weight ratio.

montmorillonite modified with dimethyl dihydrogenated tallow quaternary ammonium chloride. PGN (aspect ratio: 300–500, quat concentration: 120 mequic/100 g, density: 2.60 g/cm^3) was purchased from NANOCOR. Modified PGN (MPGN) is a natural montmorillonite modified with dimethyl distearylammonium chloride (X-ray d_{001}: 3.41 nm).

Sample Preparation

PET and PETG were molten and blended with clay (Table I) in a twin-screw extruder (Werner and Pflederer, Model-ZSK 26 MEGAcompounder) with co-rotating and intermeshing in 26 mm and L/D ratio of 56. The PET/clay and PET/PETG/clay nanocomposites were fabricated at a barrel temperature of 230–260°C and a screw speed of 500 rpm. The extruded strands were palletized and dried at 70°C for about 24 h. These blended pellets were then dried at 100°C for 12 h. All the test specimens were prepared by an injection molding machine (Fu Chun Shin Machinery Manufacture, model-HT 100). The injection temperature profile was zone 1, 230°C; zone 2, 240°C; zone 3, 250°C; and zone 4, 260°C, and mold temperature was 35°C.

TEM Observations

A HITACHI H7500 transmission electron microscope (TEM) was used to evaluate the dispersion condition of clay. The thin foil TEM specimens were prepared by microtome with a diamond knife, and examined in TEM operated at 120 kV.

XRD Measurements

X-ray diffraction (XRD) measurements were conducted on a Rigaku D/Max RC X-ray diffractometer using Cu $K\alpha$ radiation ($\lambda = 1.5418$ Å) at 40 kV and 100 mA with a scanning rate of 2°/min.

DSC Measurement

Differential scanning calorimetry analysis (DSC) was performed using a TA apparatus (model No. Q2000). The weights of specimens used in the DSC scan are 4–5 mg. The test was first heated from 30 to 280°C at a heating rate of 5°C/min under nitrogen atmosphere.

POM Observations

A Nikon Optiphot-Pol universal stage polarizing optical microscope (Tokyo, Japan) was used to observe the spherulite morphologies of neat PET, PET/clay, PET/PETG, and PET/PETG/clay under isothermal crystallization. A thin piece of sample was sandwiched between two glass coverslips and placed on a digital hot-stage under nitrogen atmosphere. The hot-stage was rapidly heated to 300°C and held for 3 min to erase the thermal history of specimens. Then, the neat PET, PET/clay, PET/PETG, and PET/PETG/clay melts were quenched to the pre-determined crystallization temperatures and kept at these temperatures for observations.

Dynamic Mechanical Analysis

Glass transition temperatures (T_g), storage modulus at 25°C (E'_{25}), and tan δ of the PET, PETG, PET/PETG blend, and their nanocomposites were measured using a dynamic mechanical analyzer (DMA, TA Q800). The specimens were trimmed to 6 mm width × 30 mm length × 2 mm thickness. A tension mode testing was applied during the DMA scans, and the scanning range was from 0 to 250°C at a heating rate of 5°C/min and at a frequency of 1 Hz under nitrogen atmosphere.

Mechanical Properties

Tensile modulus (E) was measured by a Universal Tensile Tester with a tension velocity of 25 mm/min in compliance with the specifications of ASTM D638 (dumb-bell shaped specimens with a thickness of 2 mm). Notched Izod impact (IS) tests were carried out at ambient conditions according to the ASTM D256 standard method (10.2 mm width × 4.2 mm thickness with 2 mm notched depth).

Oxygen and Water Vapor Transmission Measurements

The transmission rates (oxygen and water vapor) were measured by Mocon OX-TRAN Model 2/61 universal apparatus. Oxygen transmission rate (OTR) was according to ASTM D 3985, 40°C and 0% relative humidity (RH). Water vapor transmission rate (WVTR) was according to ASTM F 1249, 40°C and 100% RH. The specimen test area and thickness were 5 cm^2 and 0.6 mm, respectively, for all specimens.

Optical Properties

Total light permeation coefficient (T) were measured by a Haze/Turbidimeter (Nippon Denshoku Industries, Japan, model No. NDH 2000) according to the ISO 14782 methods (specimen thickness, 2 mm).

RESULTS AND DISCUSSION

TEM Observations

Figure 1 presents the distribution of the organoclay in the PET, PETG, and PET/PETG matrices. The dispersion of clay in the PET matrix [Figure 1(a)] is mostly in homogeneous distribution with domain dimension being less than 10 nm; however, there are a few fillers dispersing in intercalation with domain dimension being up to 25 nm. The domain dimension for the PETG/clay [Figure 1(b)] seems to be larger than that of the PET/clay, and it is mostly less than 25 nm; occasionally, it may be up to 50 nm. The domain dimension for the PET/PETG/clay [Figure 1(c)] is mostly in 25–50 nm. This suggests that the organoclay in the PET, PETG, and PET/PETG blend would be in the intercalation morphology.

XRD Analysis

In our previous study, we have proved that the dispersion of organoclay in PET/PETG matrix could be in intercalation distributions.[22] The specimens containing PET polymer (i.e., PET,

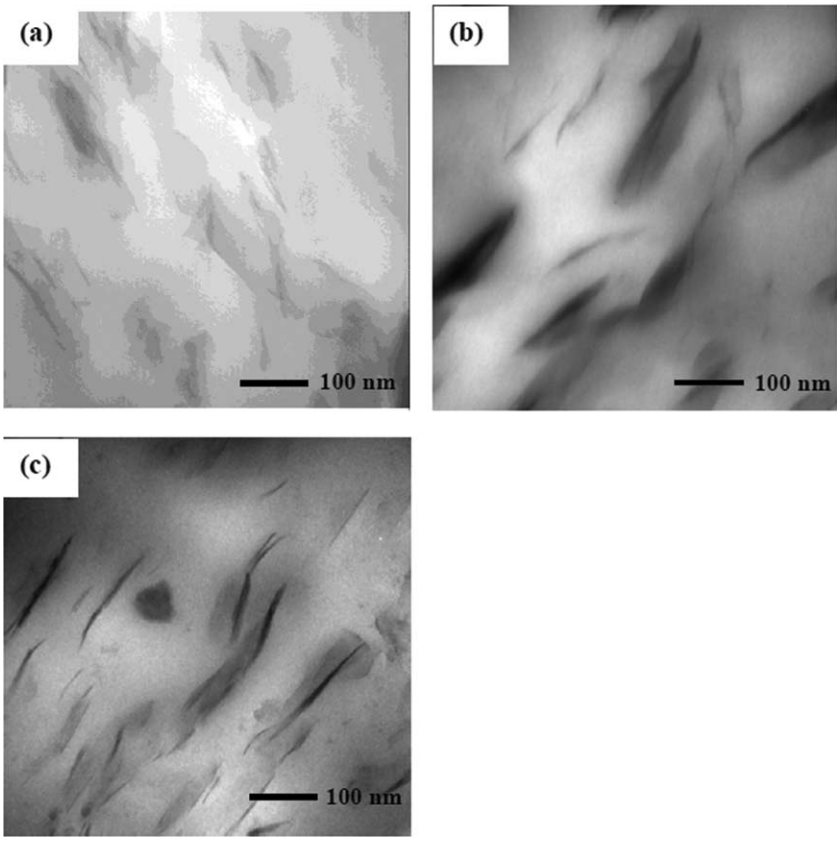

Figure 1. TEM micrographs of the organoclay in the polymer matrices: (a) PET/clay, (b) PETG/clay, and (c) PET/PETG/clay.

PET/clay, and PET/PETG/clay) exhibited similar diffraction peaks over the entire range of scans, indicating that the introduction of the clay did not affect the crystal structure of the PET polymer. The crystal structure of PET is a well-known triclinic unit cell.[24] The PET/PETG (50/50) blend significantly decreased the intensities at all diffraction peaks, indicating that mixing the PET with the amorphous PETG could inhibit the crystallization process of a neat PET polymer. Regarding the intensities of the diffraction peaks for the samples shown in Figure 2, the diffraction peaks for the PET/clay were more intense than those of the neat PET and PET/PETG/clay, indicating that the inclusion of the clay could increase the crystallinity of the PET polymer, as was achieved in the PET/PETG blend.

DSC Measurements

In our previous study, we have study the isothermal crystallization behavior and kinetics of the PET/PETG/clay nanocomposite.[22] In practical applications, the cold crystallization process might be occurred, so that it is necessary to conduct the cold crystallization process and to study how the clay will affect the crystallization behavior during the cold crystallization process. To investigate the effects of the inclusion and distribution of the clay on the crystallization behavior of the PET and PET/PETG blend, we conducted the cold crystallization process shown in Figure 3. The endothermic melting peak of the PET/clay is greater than that of the neat PET and PET/PETG, indicating that the inclusion of the clay could increase the crystallinities of the PET and PET/PETG matrices under the cold crystallization process, which is consistent with the XRD results. The melting temperatures (T_m) for the PET, PET/clay, PET/PETG, and PET/PETG/clay under cold crystallization process are 256.9, 258.9, 250.8, and 253.0°C, respectively. High T_m values indicate a well-developed spherulitic morphology. To investigate the effect of the clay on the spherulitic morphology of the PET/clay, PET/PETG, and PET/PETG/clay, all specimens were isothermally crystallized for 1 min at 215, 185, and 195°C, respectively, and a polarized optical microscope (POM) was used to observe the spherulitic morphologies (Figure 4). The PET

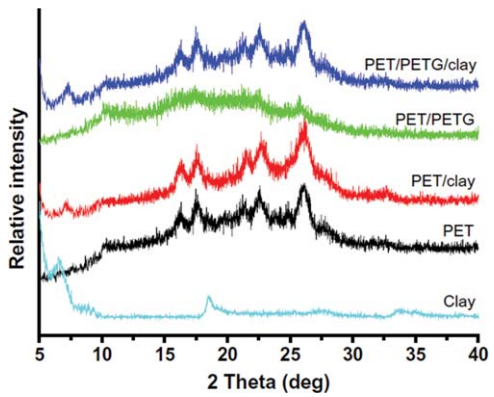

Figure 2. X-ray diffraction patterns of clay, PET, PET/clay, PET/PETG, and PET/PETG/clay. [Color figure can be viewed in the online issue, which is available at wileyonlinelibrary.com.]

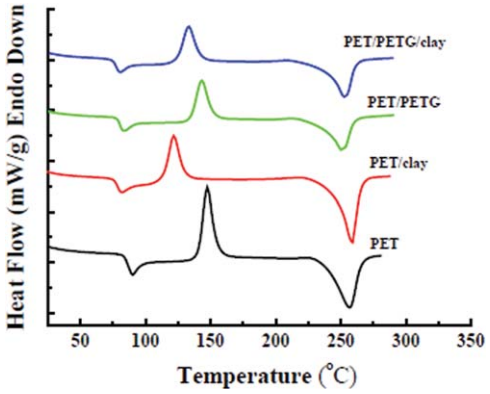

Figure 3. DSC heating traces of PET, PET/clay, PET/PETG, and PET/PETG/clay. [Color figure can be viewed in the online issue, which is available at wileyonlinelibrary.com.]

spherulites in the PET/clay [Figure 4(a)] appeared more frequently than those in the PET/PETG [Figure 4(b)] and PET/PETG/clay [Figure 4(c)]; furthermore, the spherulitic morphology was relatively more developed in the PET/clay. The crystallites in the PET/PETG blend exhibited fewer crystallizable units, although the spherulite dimensions were larger than those in the PET/clay composite. However, blending the PET with the amorphous PETG caused the Maltese-cross pattern and the crystallite boundary of PET polymer to almost disappear and become distorted, compared to that of the PET/clay. Furthermore, the PET/PETG/clay exhibited a rod-like or disc-like crystallite morphology, from which the Maltese-cross pattern disappeared completely. The clay induced heterogeneous nucleation during the cold crystallization process. This is consistent with our previous study on the isothermal crystallization of PET/clay and PET/PETG/clay.[22]

Thermomechanical Properties

As reported, nanofillers can increase the bulk modulus with a simultaneous decrease in the damping factor (tan δ) of the resulting polymer nanocomposites.[25–28] In order to investigate the effect of the organoclay on the thermomechanical behavior of PET/PETG matrix, a dynamic mechanical analyzer was used to determine the thermomechanical properties, including storage modulus, tan δ, and glass transition temperature of the PET/PETG/clay nanocomposite. Figure 5 shows the thermomechanical properties of the PET, PETG, PET/PETG blend, and their nanocomposites. The Young's modulus (E), storage modulus at 25°C (E'_{25}), tan δ maximum values (tan δ_{peak}), glass transition temperatures (T_g), and impact strength (IS) of these specimens are shown in Table II. As discussed, the inclusion of the clay into the PET and PET/PETG blend potentially imparts a greater number of crystallization sites into the PET and PET/PETG matrices; consequently, the crystallinities of these matrices can increase compared to those of the neat PET and PET/PETG blend. Accordingly, the incorporation of the clay could substantially increase the E'_{25} values of the PET, PETG, and PET/PETG blend. The E and IS values for these polymers exhibited an identical trend. However, blending the PET with the PETG caused the tough PET polymer to soften; when the PETG was introduced, both the E and IS values were lower than those of the neat PET. The damping factor (tan δ) is obtained by dividing the loss modulus by the storage modulus (E''/E'); a high value indicates a soft polymer. In this study, we used tan δ_{peak} to estimate the damping property of the PET, PETG, PET/PETG blend, and their nanocomposites (Figure 5 and Table II). Previous studies have proposed that nanofillers can simultaneously increase the bulk modulus and decrease the tan δ of the

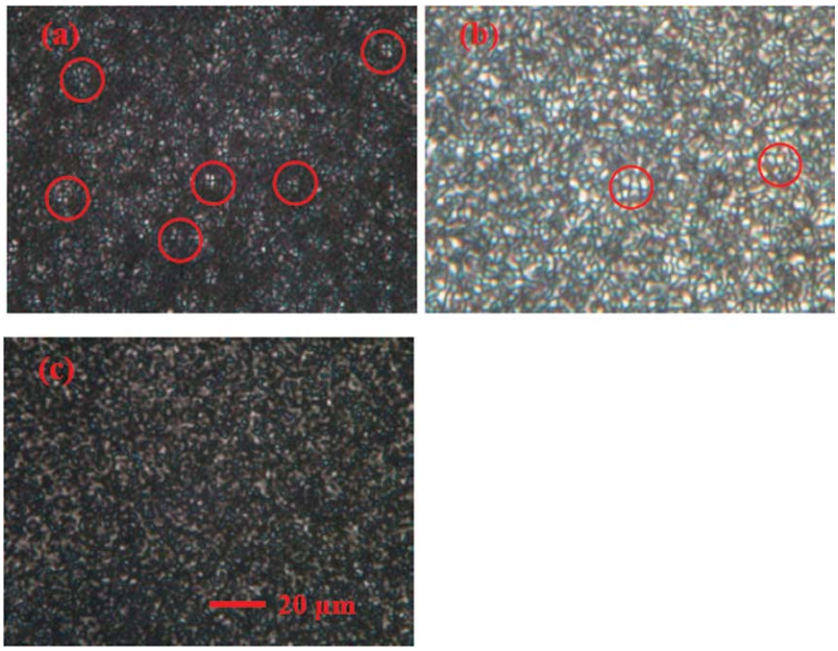

Figure 4. The spherulite morphologies of (a) PET/clay, (b) PET/PETG, and (c) PET/PETG/clay at 215, 185, and 195°C, respectively, for 60 s. The circled in the pictures are the spherulite morphology of PET polymer. [Color figure can be viewed in the online issue, which is available at wileyonlinelibrary.com.]

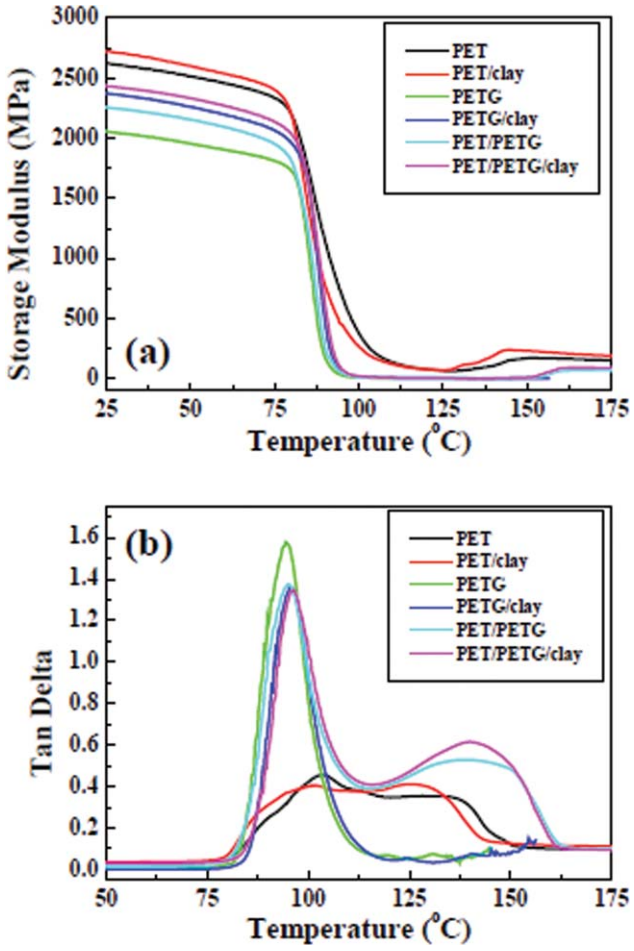

Figure 5. The thermomechanical properties of PET, PET/clay, PETG, PETG/clay, PET/PETG, and PET/PETG/clay composites. (a) Storage modulus and (b) damping factor (tan δ) spectra. [Color figure can be viewed in the online issue, which is available at wileyonlinelibrary.com.]

resulting polymer nanocomposites.[25–28] In this study, the clay decreased the tan δ_{peak} values of the PET and PETG, and blending the PET with the amorphous PETG increased the tan δ_{peak} value of the PET. Except for the neat PETG and PETG/clay, the specimens containing crystalline PET (PET, PET/clay, PET/PETG, and PET/PETG/clay) exhibited broadening crystallization peaks ranging from 125 to 160°C. The event in the dynamic mechanical analysis (DMA) measurement is consistent with that in the differential scanning calorimetry (DSC) heating trace shown in Figure 3.

Tsagaropoulos and Eisenberg filled poly(dimethylsiloxane) (PDMS) and styrene–butadiene-rubber (SBR) with silica particles (diameter = 7 nm); consequently, the silica particles increased the T_g values of the formed PDMS/silica and SBR/silica composites.[18] However, the silica particles in polystyrene (PS) and poly(methyl methacrylate) (PMMA) decreased the T_g values of the formed PS/silica and PMMA/silica composites. Tien and Wei asserted that the nano-sized layered silicate from montmorillonite can substantially increase the hard segment phase of polyurethane (PU).[29] In this study, we used the tan δ_{peak} values to define the T_g values of the PET, PETG, PET/PETG blend, and their nanocomposites (Table II). Clay in 6 phr decreased the T_g value by 1.9°C from 103.5°C (PET) to 101.6°C (PET/clay). However, it increased the T_g values of the PETG/clay (100/6) and PET/PETG/clay (50/50/6) by approximately 1.1°C and 1.0°C, respectively. As discussed, the *E* and *IS* values for the amorphous PETG are 2184 MPa and 1.55 J/m, respectively, and those for the crystalline PET are 2394 MPa and 2.70 J/m, respectively. The nanofillers appeared to increase the T_g values of the soft polymers, although they decrease the T_g values of the tough polymers, which is consistent with the assertion made by Tsagaropoulos and Eisenberg.[25]

Barrier Properties

It is well known that the inclusion of nanofillers can improve the gas-barrier properties against oxygen and water vapor of the resulting composites. Tsai et al. proposed that the PETG/clay composites can improve both the oxygen transmission rate (OTR) and water vapor transmission rate (WVTR) because of the longer path for gas to diffuse through the nanocomposites caused by the inclusion of the clay.[20] In this study, we prepared PET/clay, PETG/clay, and PET/PETG/clay nanocomposites, and investigated the properties of OTR and WVTR among the PET, PETG, PET/PETG blend and their nanocomposites (Figure 6). The OTR and WVTR values yielded by the amorphous PETG were greater than those from the crystalline PET. Compared with the neat PETG, blending the PETG with the crystalline PET improved the gas-barrier properties, as shown by the reduced OTR and WVTR. Furthermore, incorporating the clay into the PET, PETG, and PET/PETG blend substantially reduced their OTR and WVTR values. Compared to the unfilled PET, PETG, and PET/PETG blend, the incorporation of 6 phr clay reduced the OTR values by 38, 13, and 28%, respectively. The

Table II. The Tensile Modulus (*E*), Storage Modulus at 25°C (E'_{25}), Tan Delta Peak (tan δ_{peak}), Glass Transition Temperature (T_g), and Izod Impact Strength (*IS*) of PET/PETG/Clay Nanocomposites

Sample	*E* (MPa)	E'_{25}(MPa)	tan δ_{peak}	T_g (°C)	*IS* (J/m)
PET	2394	2611	0.457	103.5	2.70
PETG	2148	2045	1.575	94.6	1.55
PET/PETG (50/50)	2232	2249	1.373	95.3	1.92
PET/clay (100/6)	2960	2718	0.407	101.6	2.81
PETG/clay (100/6)	2493	2369	1.356	95.7	1.63
PET/PETG/clay (50/50/6)	2718	2418	1.347	96.3	2.13

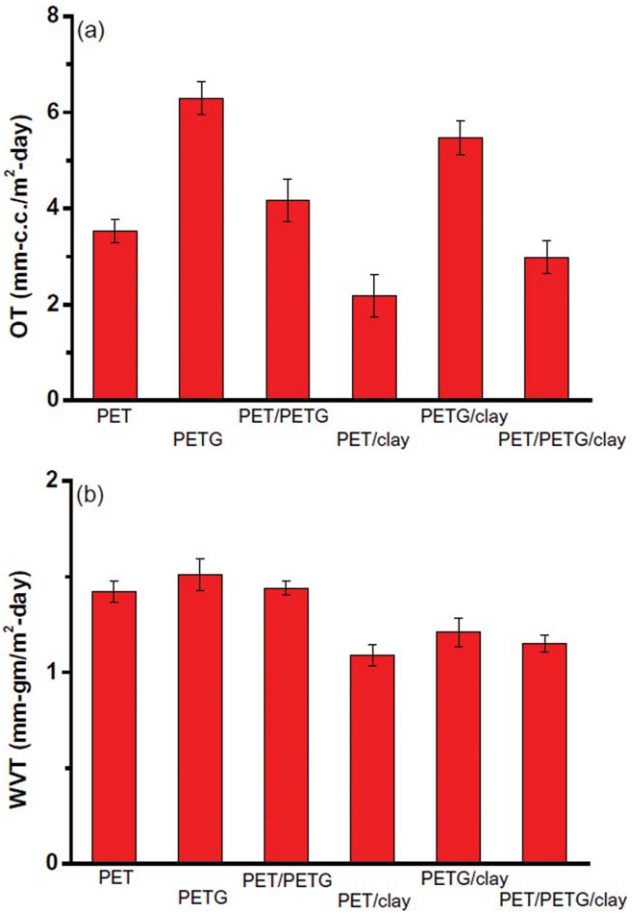

Figure 6. (a) Oxygen transmission rate (OTR) and (b) water vapor transmission rate (WVTR) of the PET, PETG, PET/PETG blend, and their nanocomposites. [Color figure can be viewed in the online issue, which is available at wileyonlinelibrary.com.]

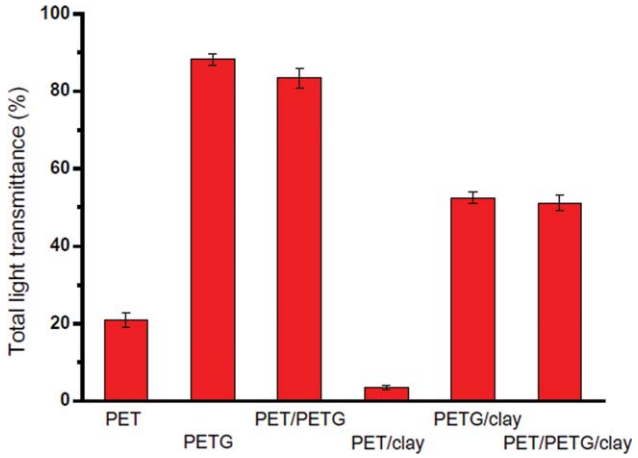

Figure 7. Optical properties of the PET/PETG/clay nanocomposites (2 mm thick). [Color figure can be viewed in the online issue, which is available at wileyonlinelibrary.com.]

OTR value for the neat PETG was 6.295 mm-cc/m^2-day, whereas that of the PET/PETG (50/50) was 4.167 mm-cc/m^2-day. Furthermore, the PET/PETG/clay progressively lowered its OTR value to 2.992 mm-cc/m^2-day. This shows that the OTR value of the PETG can be improve substantially by introducing both the crystalline PET and the clay as a nucleating agent.

Moreover, the incorporation of 6 phr clay into the PET, PETG, and PET/PETG blend reduced the WVTR values by 23, 4.6, and 16%, respectively. The WVTR value for the neat PETG was 1.511 mm-gm/m^2-day, whereas that of the PET/PETG (50/50) was 1.441 mm-gm/m^2-day. As anticipated, the PET/PETG/clay progressively lowered its WVTR value to 1.154 mm-gm/m^2-day. The trend of the WVTR was similar to that of the OTR; that is, the water vapor barrier property of the PETG can be improved by introducing both the crystalline PET and the clay as a nucleating agent.

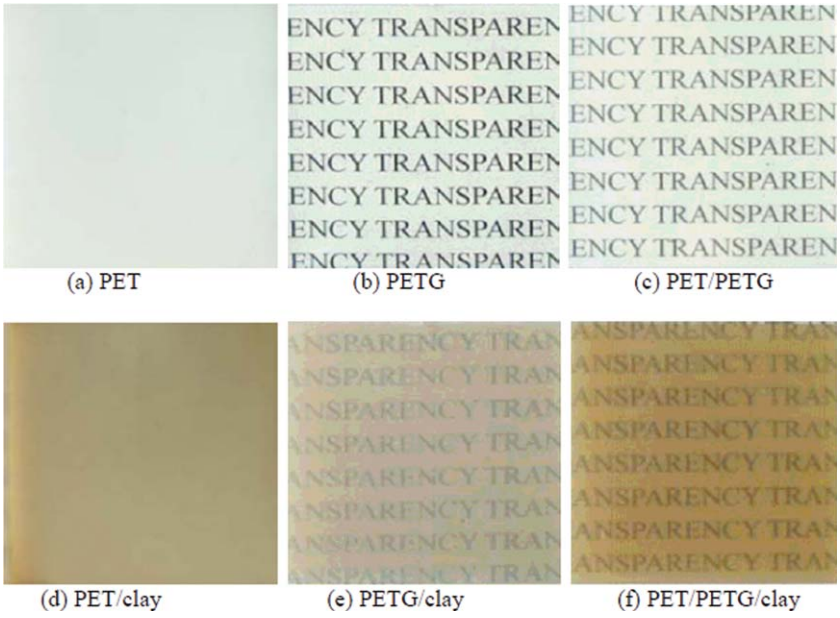

Figure 8. Transparency effects on PET blended with PETG and clay (2 mm thick). [Color figure can be viewed in the online issue, which is available at wileyonlinelibrary.com.]

Effect of Clay on the Transparency

As discussed, PET/clay nanocomposites are generally opaque because of the high crystallinity caused by the inclusion of clay. As mentioned, the inclusion of amorphous PETG can retard the crystallization process and in turn increase the light transmittance of the resulting nanocomposite. Figure 7 shows that the total light transmittance for the crystalline PET is 21%, and the inclusion of clay significantly reduces this value. However, the total light transmittance for the amorphous PETG is 88%, and blending the PETG with the PET reduces this value to 84%. The inclusion of clay reduces the total light transmittance of both the PETG and the PET/PETG blend to 52 and 51%, respectively. Figure 8 shows images depicting the transparency effects on the PET, PETG, PET/PETG blend, and their nanocomposites. As discussed, the inclusion of the clay into the crystalline PET substantially improved its gas-barrier properties, although this simultaneously induced crystallization, which increased the opacity of the formed composites. However, the incorporation of the clay into the amorphous PETG or PET/PETG blend improved both the OTR and WVTR by approximately 13.0–28.0% and 4.6–20.0%, respectively, and simultaneously maintained the transparency of the PETG and PET/PETG blend (Figure 8).

CONCLUSION

The XRD and DSC measurements indicated that the inclusion of the clay induced heterogeneous nucleation during the cold crystallization process and increased the crystallinity of the PET and PET/PETG blend. The inclusion of clay substantially increased the mechanical and thermomechanical properties (i.e., storage modulus, Young's modulus, and impact strength) of the PET, PETG, and PET/PETG blend. The clay increased the T_g value of a soft polymer (e.g., PETG), although it decreased the T_g value of a tough polymer (e.g., neat PET). Furthermore, the clay in the PET, PETG, and PET/PETG blend exhibited a substantial reduction in OTR and WVTR, thereby indicating a significant improvement in their gas-barrier properties. The inclusion of clay can make the crystallizable PET matrix crystalline opaque. However, the clay in the polymer matrix containing the amorphous and transparent PETG improved its gas-barrier properties and simultaneously maintained its transparency.

REFERENCES

1. Choi, W. J.; Kim, H. J.; Yoon, K. H.; Kwon, O. H.; Hwang, C. I. *J. Appl. Polym. Sci.* **2006**, *100*, 4875.
2. Zeng, K.; Bai, Y. *Mater. Lett.* **2005**, *59*, 3348.
3. Kim, S. H.; Kim, S. C. *J. Appl. Polym. Sci.* **2007**, *103*, 1262.
4. Tsai, T. Y.; Li, C. H.; Chang, C. H.; Cheng, W. H.; Hwang, C. L.; Wu, R. *J. Adv. Mater.* **2005**, *17*, 1769.
5. Hamzehlou, S. H.; Katbab, A. A. *J. Appl. Polym. Sci.* **2007**, *106*, 1375.
6. Wan, T.; Chen, L.; Chua, Y. C.; Lu, X. *J. Appl. Polym. Sci.* **2004**, *94*, 1381.
7. Calcagno, C. I. W.; Mariani, C. M.; Teixeira, S. R.; Mauler, R. S. *Polymer* **2007**, *48*, 966.
8. Wang, Y.; Shen, C.; Li, H.; Li, Q.; Chen, J. *J. Appl. Polym. Sci.* **2004**, *91*, 308.
9. Yangchuan, K.; Chengfen, L.; Zongneng, Q. *J. Appl. Polym. Sci.* **1999**, *71*, 1139.
10. Hellati, A.; Benachour, D.; Caqiao, M. E.; Boufassa, S. Calleja, F. J. *J. Appl. Polym. Sci.* **2010**, *118*, 1278.
11. Lee, S. J.; Hahm, W. G.; Kikutani, T.; Kim, B. C. *Polym. Eng. Sci.* **2009**, *49*, 317.
12. Giraldi, A. L.F.; Bizarria, M. T. M.; Silva, A. A.; Mariano, C.; Velasco, J. I.; D'Avila, M. A.; Mei, L. H. J. *J. Nanosci. Nanotechnol.* **2009**, *9*, 3883.
13. Yin, M.; Li, C.; Guan, G.; Zhang, D.; Xiao, Y. *J. Appl. Polym. Sci.* **2009**, *114*, 2327.
14. Hwang, S. Y.; Lee, W. D.; Lim, J. S.; Park, K. H.; Im, S. S. *J. Polym. Sci. Part B: Polym. Phys.* **2008**, *46*, 1022.
15. Guan, G.; Li, C.; Yuan, X.; Xiao, Y.; Liu, X.; Zhang, D. *J. Polym. Sci. Part B: Polym. Phys.* **2008**, *46*, 2380.
16. Ou, C. F.; Ho, M. T.; Lin, J. R. *J. Appl. Polym. Sci.* **2004**, *91*, 140.
17. Ou, C. F.; Ho, M. T.; Lin, J. R. *J. Polym. Res.* **2003**, *10*, 127.
18. Turner, S. R. *J. Polym. Sci. Part A: Polym. Chem.* **2004**, *42*, 5847.
19. Tsai, Y.; Fan, C. H.; Hung, C. Y.; Tsai, F. J. *J. Appl. Polym. Sci.* **2007**, *104*, 279.
20. Tsai, Y.; Wu, J. H.; Leu, M. T. *Polym. Adv. Technol.* **2011**, *22*, 2319.
21. Papadopoulou, C. P.; Kalfoglou, N. K. *Polymer* **1997**, *38*, 631.
22. Wu, J. H.; Yen, M. S.; Kuo, M. C.; Wu, C. P.; Leu, M. T.; Li, C. H.; Tsai, F. K. *J. Appl. Polym. Sci.* **2013**, *128*, 487.
23. Tsai, Y.; Jheng, L.; Hung, C. Y. *Polym. Degrad. Stab.* **2010**, *95*, 72.
24. Goschel, U. *Polymer* **1996**, *37*, 4049.
25. Tsagaropoulos, G.; Eisenberg, A. *Macromolecules* **1995**, *28*, 396.
26. Tsagaropoulos, G.; Eisenberg, A. *Macromolecules* **1995**, *28*, 6067.
27. Arrighi, V.; McEwen, I. J.; Qian, H.; Serrano Prieto, M. B. *Polymer* **2003**, *44*, 6259.
28. Ray, S. S.; Yamada, K.; Okamoto, M.; Ueda, K. *Polymer* **2003**, *44*, 857.
29. Tien, Y. I.; Wei, K. H. *J. Appl. Polym. Sci.* **2002**, *86*, 1741.